

We are IntechOpen, the world's leading publisher of Open Access books Built by scientists, for scientists

6,900

Open access books available

186,000

International authors and editors

200M

Downloads

Our authors are among the

154

Countries delivered to

TOP 1%

most cited scientists

12.2%

Contributors from top 500 universities



WEB OF SCIENCE™

Selection of our books indexed in the Book Citation Index
in Web of Science™ Core Collection (BKCI)

Interested in publishing with us?
Contact book.department@intechopen.com

Numbers displayed above are based on latest data collected.
For more information visit www.intechopen.com



Numerical study of backward extrusion process using finite element method

K.Abrinia and S.Orangi

*School of Mechanical Engineering, College of Engineering,
University of Tehran, I.R.Iran*

1. Introduction

One of the important bulk forming processes which has a lot of applications is the backward extrusion that has been the subject of study of researchers for many years. This process is very useful for making shaped sections with closed ends or integrated parts which are hard to produce by means of other processes. Numerical analyses of bulk forming processes are difficult to perform due to the large deformations occurring during the material flow which causes heavy mesh distortions. However for those bulk forming processes which have a non steady state nature like the backward extrusion of shaped sections this difficulty increases. The amount of previous works on the numerical study of backward extrusion is therefore much less as compared with analytical research carried in the same area. Here are given a review of a few numerical analyses for the backward extrusion and then some of the analytical works would be examined as well.

Im et al (2004) gave an account of a FEM analysis for a test which was used to determine the friction factor for the bulk forming processes. This was called a tip test. In their study, a set of tip tests was carried out to determine the friction condition for the backward extrusion process of aluminum alloy. It had been experimentally observed that the radial distance from the tip to the side wall of the specimen increased with higher level of frictions and thus could be used as an effective measure of the friction condition. It was also found that the radial tip position was more sensitive to the change of friction condition at the punch than the die and that the global average friction level at the punch interface was higher than that at the die interface. Finite element simulation results also clearly confirmed that the relationships among the radial tip distance, forming load and shear friction factor were linear. Shin et al (2005) presented a new approach to process optimal design in non-isothermal, non-steady metal forming process. They investigated the development of a finite element-based approach for process optimization in forming of a difficult-to-form materials, such as titanium alloys. Due to strong dependence of the flow stress of these materials on temperature, interaction between deformation and heat transfer in the workpiece and contact heat transfer between the tool and the workpiece were rigorously reflected in the proposed approach. Also reflected was the effect of remeshing, which was essential for the treatment of a complex-shaped product. Consequently, the main merit of the proposed approach was that the diverse process parameters that could be treated as design variables,

and the applicability was not affected by the shape complexity of the product. Saboori et al (2006) presented a finite element solution for the backward extrusion process using ABAQUS commercial software. They investigated the effect of the die radius on the extrusion pressure and obtained an optimum design. In a similar paper to above Bakhshi-Jooybari et al (2006), based on the slab method and an iterative algorithm, obtained the optimum die profile in backward rod extrusion of lead. Furthermore, by using the finite element software, ABAQUS, the optimum die angle for conical die was determined. Uyyuru and Valberg (2006) studied the material flow of aluminum-alloy slug over the punch head in backward cup extrusion process by physical modeling technique combined with FE-simulations. Specially designed intrinsic tube/circle pattern made of contrast material was used for the purpose. New physical pattern technique was very useful as it allowed calculation of the extension of surface all over the inner wall of the cup with ease. Degree of surface extension over the punch head was observed to vary along the cup length. Close to the base of the cup, extension was very high compared with extension at top of the cup. Long (2006) investigated the effects of elastic-plastic deformation and temperature variations of the workpiece and tools on dimensional errors of a cold backward extruded cup. He developed a finite element analysis procedure to predict component dimensional deviations during different stages of the cold extrusion process. In an entire cold forming cycle, the material plastic deformation, heat generation, temperature distribution and tool elastic deformation in backward cup extrusion were obtained, which enabled a quantitative evaluation of the dimensional errors of the cold formed component with a view to the effects of forming stages on dimensional errors of the extruded cup. Abrinia and Gharibi (2008) investigated the backward extrusion of thin wall cups using FEM. In this investigation the extrusion pressure, the forces acting on the punch head and the thickness of the walls were studied while the shape of the punch head was varied using different profiled curves. It was shown that smaller and more uniform can wall thickness could be achieved by using a proper punch head profile.

As could be seen from the literature review of the previous work the finite element analyses of backward extrusion has been centered on products such as cups which are fairly simple geometrical shapes with axisymmetric nature. However considering the FEM analyses of the backward extrusion of shaped sections, with its three dimensional material flow, barely any relevant works could be seen in the literature and that is why the rest of this section deals with the review of the works involving upper bound and other non numerical methods.

Bae and Yang (1992) gave an account of an upper-bound method to determine the final-stage extrusion load and the deformed configuration for the three-dimensional backward extrusion of internally elliptic-shaped tubes from round billets. In another article, Bae and Yang (1993-a) presented a simple kinematically admissible velocity field for the backward extrusion of internally circular shaped tubes from arbitrarily shaped billets. They carried out experiments with full annealed aluminum alloy billets at room temperature using four circular-shaped punches. Another new kinematically admissible velocity field was proposed by Bae and Yang (1993-b) to determine the final-stage extrusion load and the average extruded height in the backward extrusion of internally non axisymmetric tubes from round billets. Lee and Kwan (1996) presented a modified kinematically admissible velocity field for the backward extrusion of internally circular-shaped tubes from arbitrarily shaped billets. From the proposed velocity field, the upper-bound extrusion load and average extruded

height for regular polygon shaped billets were determined with respect to the chosen parameters. A new upper-bound elemental method was proposed by Lin and Wang (1997) to improve the ineffectiveness of the upper bound elemental technique (UBET) for solving forging problems that were geometrically complex or needed a forming simulation for predicting the profile of the free boundary. An upper-bound formula was developed to analyze the backward extrusion forging of regular polygon cup-shaped components in an article by Moshksar and Ebrahimi (1998). Guo et al (2000) analyzed two- and one-way axisymmetric hot backward extrusion problems by a combined finite element method. A finite element simulation for the backward extrusion of internally hollow circular sections from polygonal billets was performed by Abrinia and Orangi (2007). In this article, investigation of process parameters for the backward extrusion of arbitrary-shaped tubes from round billets was carried out using finite element approach.

The purpose of this work is to present a detailed study of the backward extrusion of shaped sections including circular and non-circular billets using finite element method. The work presented here is based on the publications of the authors given in the references and mainly on the work by Abrinia and Orangi, 2009.

2. Theory and modeling of the Process

The theory of finite element analysis for the backward extrusion process is presented here and subjects like analysis step, interaction, boundary condition and meshing are dealt with.

2.1 Analysis steps

A sequence of one or more analysis steps can be defined within a model. The step sequence makes a way to change the loading and boundary conditions of the model, changes in the way parts of the model interact with each other and the addition or removal of parts. In addition, steps allow changing the analysis procedure, the data output, and various controls. Steps may be used to define linear perturbation analyses about nonlinear base states.

The initial step allows one to define boundary conditions, predefined fields, and interactions that are applicable at the beginning of the analysis.

The initial step is followed by one or more analysis steps. Each analysis step is related with a specific procedure that defines the type of analysis to be performed during the step, such as a static stress analysis or a transient heat transfer analysis. One can change the analysis procedure from step to step in any desired way, so, there will be great flexibility in performing the analyses. Considering the fact that the state of the model (stresses, strains, temperatures, etc.) is updated throughout all general analysis steps, the effects of previous history are always included in the response for each new analysis step.

Between two main nonlinear methods of solutions that are often used in cold forming process simulations; namely the explicit dynamic and the implicit Newton incremental methods, the explicit dynamic method was chosen for all the simulations carried out in this work.

The explicit dynamic analysis method is based on the implementation of an explicit integration rule (Fig. 1) by using the diagonal or lumped element mass matrices. The basic motion equation of the body is:

$$M\ddot{u} + F(u) = 0$$

Now integrating and using the explicit central difference integration rule, we have:

$$\dot{u}^{(i+\frac{1}{2})} = \dot{u}^{(i-\frac{1}{2})} + \frac{\Delta t^{(i+1)} + \Delta t^{(i)}}{2} \ddot{u}^{(i)},$$

$$u^{(i+1)} = u^{(i)} + \Delta t^{(i+1)} \dot{u}^{(i+\frac{1}{2})},$$

where \dot{u} is the velocity and \ddot{u} is the acceleration. The superscript (i) refers to the increment number and $i - \frac{1}{2}$ and $i + \frac{1}{2}$ are middle increment values.

The use of the diagonal element mass matrices is the computational efficiency key to the explicit dynamics procedure because the inversion of the mass matrix that is used in the computation for the accelerations at the beginning of the increment is trivial.

$$\ddot{u}^{(i)} = M^{-1} \cdot (F^{(i)} - I^{(i)})$$

where M is the diagonal lumped mass matrix, F is the applied load vector and I is the internal force vector.

Iterations and tangent stiffness matrix construction are not required in this procedure. The explicit procedure integrates through time by employing small time increments. The central difference operator is conditionally stable, and the stability limit for the operator (with no damping) is given by the maximum eigenvalue in the system as:

$$\Delta t \leq \frac{2}{\lambda_{\max}}$$

Its advantage is its simplicity and it is straightforward to implement. However, the disadvantages are: firstly that it is conditionally stable; i.e. it may become unstable. Secondly, the accuracy of the integration depends, of course, on the time step size, Δt . In comparison with other analysis such as static and implicit methods, the time and cost of explicit method is lower than that of the others. The reason is that the explicit method determines the solution without iterating and it doesn't require large numbers of time increments such as the case for the static analysis. These are the most important advantages when dealing with large deformations such as the one for the backward extrusion process.

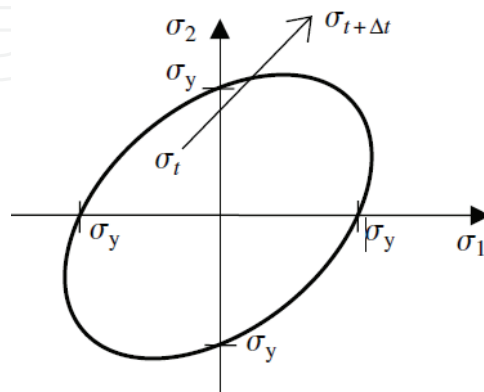


Fig. 1. Schematic representations of explicit integration using the radial return method, of Von Mises plasticity equations (Wriggers, 2008).

2.2 Interaction (friction)

Cold forming process systems involve contact between the work piece and the tools. Contact itself is a typical type of nonlinear boundary conditions encountered in finite element analysis. Contact conditions are a special class of discontinuous constraints allowing forces to be transmitted from one part of the model to another. This constraint is discontinuous because it is applied only when two surfaces are in contact. When the two surfaces are separated, no constraint is applied.

The interaction between contacting surfaces consists of two components: one normal to the surfaces and the other tangential to the surfaces. The tangential component consists of the relative motion (sliding) of the contacting surfaces and associated frictional shear stresses.

In addition to determining whether contact has occurred at a particular point, the analysis also must calculate the relative sliding of the two surfaces of the contact pair and their tangential interaction. There exist two sets of formulations in contact modeling: small sliding and finite sliding formulations. Small sliding formulation is used when the magnitude of sliding is small. In contrast, finite sliding formulations are used when the magnitude of sliding is large and finite. It is much less expensive computationally to model problems where the sliding between the surfaces is small. Finite sliding is the most general and allows arbitrary motion of the surfaces forming the contact pair. In cold forming process simulation, since usually there is large relative motion between the work piece and tools due to the punch and tool movement or because of deformation and shape changes of the work piece, the finite sliding model is often used between them. Small sliding model can be used between two tools where there is no or little relative motion.

Coulomb friction is the friction model used to describe the interaction of contacting surfaces. In the basic form of the Coulomb friction model, two contacting surfaces can carry shear stresses up to a certain magnitude across their interface before they start sliding relative to one another; this state is known as sticking. The Coulomb friction model defines this critical shear stress, τ_{crit} , at which sliding of the surfaces starts as a fraction of the contact pressure, p , between the surfaces ($\tau_{crit} = \mu p$). The stick/slip calculations determine when point transition from sticking to slipping or from slipping to sticking occurs. The fraction, μ , is known as the coefficient of friction. The basic friction model assumes that μ is the same in all directions (isotropic friction). For a three-dimensional simulation there are two local orthogonal components of shear stresses, τ_1 and τ_2 , along the interface between the two bodies. We may combine the two shear stress components into an equivalent shear stress, $\bar{\tau}$, for the stick/slip calculations, where $\bar{\tau} = \sqrt{\tau_1^2 + \tau_2^2}$. In addition, the two slip

velocity components can be combined into an equivalent slip rate, $\sqrt{\dot{\gamma}_1^2 + \dot{\gamma}_2^2}$.

There are three contact algorithms used in ABAQUS. The first one is an algorithms used in the standard analysis and built around the Newton-Raphson technique. The second one is a kinematic contact algorithm and the third one is a penalty contact algorithm. The second and third algorithms mentioned above are used in ABAQUS/explicit. ABAQUS/explicit uses a kinematic contact formulation that achieves precise compliance with the contact conditions using a predictor/corrector algorithm. We applied penalty contact algorithm in our simulations because it is more sensitive to element distortion than the kinematic

algorithms. In ABAQUS software, contact is determined by defining two surfaces namely the slave and the master surfaces. Contact is applied on slave nodes (101,102,103) and master nodes (1,2,3). In the case of work piece and die, work piece is considered as slave and die as master (Fig. (2)).

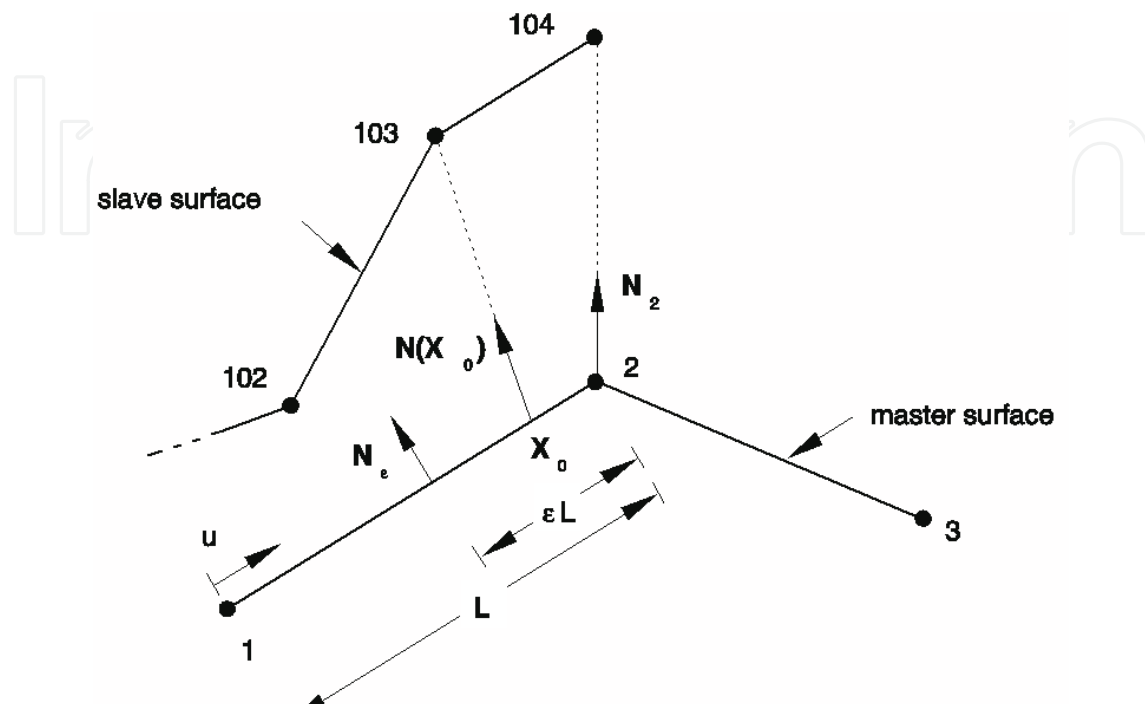


Fig. 2. Slave and master surfaces

The constitutive behavior in tangential direction is very complex. It depends on many factors such as surface roughness, magnitude of the normal pressure, tangential relative velocities, contaminants or humidity, etc. This complexity can be shown by the constitutive equations which then depend on many material parameters. Since it is not easy to determine such parameters, the simplest constitutive relation, the so-called Coulomb law is employed in many engineering applications which only depend upon one material parameter, the coefficient of friction. However, depending on the material pairing, there exist many variants of this constitutive relation for the tangential stresses.

2.3 Load (boundary condition):

Boundary condition can be used to specify the values of all basic solution variables (displacements, rotations, warping amplitude, fluid pressures, pore pressures, temperatures, electrical potentials, normalized concentrations, acoustic pressures, or connector material flow) at nodes;

There are various ways to define boundary conditions in finite element. These are based on the followings:

- Symmetry/Anti-symmetry
- Displacement/Rotation
- Velocity/Angular velocity
- Acceleration/Angular acceleration
- Connector displacement or velocity or acceleration

We have implemented velocity/ angular velocity as the boundary condition. The definition is given in terms of the angular velocity instead of the total rotation if velocity-type boundary conditions are used to prescribe rotations.

2.4 Meshing

Behavior of an element is characterized by five aspects, namely: family, degrees of freedom (directly related to the element family), number of nodes, formulation and integration. The fundamental variables calculated during the analysis are the degrees of freedom. For a stress/displacement simulation the degrees of freedom are the translations.

2.5 Three dimensional elements

Three-dimensional elements are defined in the global X, Y, and Z space. These elements are utilized when the geometry and or the applied loading are too complex for any other element type with fewer spatial dimensions.

2.5.1 Stress/displacement elements

Stress/displacement elements are used in the modeling of linear or complex nonlinear mechanical analyses that may involve contact, plasticity, and/or large deformations. Stress/displacement elements can be used in the following analysis types: static and quasi-static analysis, implicit transient dynamic, explicit transient dynamic, modal dynamic, and steady-state dynamic analysis, so, we chose stress/displacement elements for the analysis. Hence, we used stress/ displacement elements in our modeling.

In explicit analysis, triangular, tetrahedral, and wedge elements can be used. Solid elements can include first- and second-order triangles, tetrahedral, and wedge elements for planar, axisymmetric, and three-dimensional analysis.

Triangular and tetrahedral elements are utilized in automatic meshing algorithms. These elements ease meshing process of complicated shapes and they are common in general applications. The disadvantage of these elements is that they are less sensitive in distortion. In contrast, hexahedral and quadrilateral elements have high accuracy computationally. Besides these elements have good performance and accuracy because of their sensitivity to distortion. In addition, hexahedral and quadrilateral elements have good convergence in comparison with tetrahedral and triangular ones. This is the reason that in the present analysis hexagonal elements have been used to analyse the backward extrusion of aluminum alloys.

2.5.2 Adaptive meshing

Backward extrusion process involves large amounts of permanent deformation. This high degree of deformation may cause problems during the finite element simulation. The analysis may easily end as a result of severe mesh distortion. Therefore, the special meshing techniques are required to analyse these problems. Adaptive meshing and remeshing or rezoning are two solutions to these problems.

Remeshing or rezoning: when the mesh is distorted severely one can pause the process of analysis and then by creating new mesh and mapping the solution onto the new mesh, the analysis will continue. For instance in mesh control one can change the amount of distortion

in terms of the length ratio (i.e. the ratio of the length of the initial mesh to that of the distorted mesh) that is one can control distortion during the process.

Adaptive meshing is another powerful tool used to maintain high-mesh quality throughout the process of analysis. Without changing the mesh topology, adaptive meshing moves the nodes only. For cases of large deformation, the mesh is allowed to move independently of the material and thus keeps away from excessive distortions. In addition, in regions where large gradients are more probable to occur, adaptive meshing allows the mesh to be refined automatically in those regions. The refining algorithm is as given below:

- Select an appropriate initial mesh which approximates the geometry of the problem accurately.
- Solve the discrete problem.
- Compute error estimators or error indicators.
- Test, whether the global error lies within the given tolerance.
- If yes, the computation is finished.
- If no, a new mesh has to be created.
- Throughout this process the former computed deformations and internal variables have to be projected onto the new mesh.

3. Modelling the Material Behaviour

This section presents the models for the behavior of the material and its definition in the FEM environment. Other FEM parameters which influence the modeling behavior will also be discussed. The following topics are covered:

- ✓ The part module
- ✓ The property module
- ✓ The Assemble module
- ✓ The step module
- ✓ The interaction module
- ✓ The load module
- ✓ The mesh module
- ✓ The job module.

3.1 The part module

In the part module, one can model geometrically the parts such as the container, die, work piece and the punch or may import parts modeled in other modeling software. Punches, containers and billets were modeled in various shapes. In all cases, billets were modeled deformable, 3D and extrusion option was used for this modeling. For elliptical, rectangular, and hexagonal tubes, the diameter of circular billet was 25 mm with a length of 25 mm. Besides, billet dimensions for the AA1100-O were 22 mm width from side to side and 20 mm length.

3.2 The property module

The property module performs the following tasks:

- Defines the materials.
- Defines the beam section profiles.

- Defines the sections.
- Assigns sections, orientations, normals, and tangents to the parts.
- Defines the composite layups.
- Defines skin reinforcement.
- Defines inertia (point mass, rotary inertia, and heat capacitance) on a part.
- Defines springs and dashpots between two points or between a point and ground.

Material definition: in all models, material was considered as Von Mises rigid-plastic material with isotropic hardening. Aluminum AA2024-O and AA1100-O were chosen as the working material. The material properties for the simulated models were assumed as follows:

For AA2024-O [2]: $\bar{\sigma} = 292.77 \times \bar{\epsilon}^{0.15} (Mpa)$

$$\rho = 2780(kg / m^3)$$

$$E = 73.1(Gpa)$$

$$\nu = 0.33$$

$$\sigma_y = 78.5(Mpa)$$

And for AA1100-O:

$$\bar{\sigma} = 136 \times \bar{\epsilon}^{-0.254} (MPa)$$

$$\rho = 2715(Kg / m^3)$$

$$E = 68.9(GPa)$$

$$\nu = 0.33$$

$$\sigma_y = 34.5(MPa)$$

The billet was modeled as a von Mises rigid-plastic material with isotropic hardening material property and the extrusion container and die were modeled as perfectly rigid.

3.3 The assembly module

After geometrical modeling and assigning properties to parts, if it is necessary to assemble them, assembling is performed in the assembly module. For instance, the gap between container and billet and the distance between punch and billet for the beginning of the process were adjusted here. These dimensions were assumed 0.2 mm and 0.5 mm respectively.

3.4 The step module

Step module tasks are:

- Creating analysis steps
- Specifying output requests
- Specifying adaptive meshing
- Specifying analysis controls
- Creating analysis steps

The time of the process, type of analysis; as an example, stress/displacement were taken in this part.

3.5 Interaction module

The Interaction module is used to define and manage the following objects:

- Mechanical and thermal interactions between regions of a model or between a region of a model and its surroundings.
- Analysis constraints for the regions of a model.
- Assembly-level wire features, connector sections, and connector section assignments to model connectors.
- Inertia (point mass, rotary inertia, and heat capacitance) on regions of the model.
- Cracks on regions of the model.
- Springs and dashpots between two points of a model or between a point of a model and ground.

In our model, contact was chosen as mechanical interaction, tangential behavior with penalty formulation. The friction factors, 0.1 and 0.2 are used for all models.

3.6 The load module

The load module is used to define and manage the following prescribed conditions:

- Loads
- Boundary conditions
- Predefined fields

In our model, the blank was constrained along its base in the z-direction and at the axis of symmetry in the r-direction. Radial expansion was prevented by contact between the blank and the die. The punch and the die were fully constrained, with the exception of the prescribed vertical motion of the punch.

3.7 The Mesh module

The Mesh module contains tools that allow us generating meshes on parts and assemblies created within Abaqus/CAE. Besides, there are functions that verify an existing mesh. Various levels of automation and control are available here. As with creating parts and assemblies, the process of assigning mesh attributes to the model—such as seeds, mesh techniques and element types—is feature based. As a result we can modify the parameters that describe a part or an assembly, and the mesh attributes that we specified within the mesh module are regenerated automatically.

The Mesh module ensures the following features:

- Tools for prescribing mesh density at local and global levels.
- Model coloring that shows the meshing technique assigned to each region in the model.
- Mesh controls, such as element shape, meshing technique, meshing algorithm, adaptive remeshing rule

- A tool for assigning Abaqus/Standard and Abaqus/Explicit element types to mesh elements. The elements can belong either to a model that you created or to an orphan mesh.
- A tool for verifying mesh quality.
- Tools for refining the mesh and for improving the mesh quality.
- A tool for saving the meshed assembly or selected part instances as an orphan mesh part

Element failure criteria for all models in our simulation: the optimum element size was obtained by trial and error until the appropriate aspect ratio (i.e.3) was achieved

- Type of element for the container modeled as discrete rigid:R3D8R
- Type of element for the punch modeled as analytical rigid: R3D4, A 4-node 3D bilinear rigid quadrilateral.
- Element type for the billet modeled as deformable: C3D8R, An 8-node linear brick element, reduced integration with hourglass control.
- Element Library: Explicit, 3D stress.
- Partitioning

Element shape: Hexahedral with sweep technique

In some cases during the analysis, distortion control was applied during the process which was considered as distortion length=0.5.

3.8 The Job module

Creating and managing analysis jobs are possible by the Job module and also to view a basic plot of the analysis results. We can use the Job module to create and manage adaptivity analyses as well.

Once all of the tasks involved in defining a model have been finished (such as defining the geometry of the model, assigning section properties, and defining contact), Job module is used to analyze our model. This module allows us to create a job, to submit it to Abaqus/Standard or Abaqus/Explicit for analysis, and to monitor its progress. If desired, creating multiple models and jobs and running and monitoring the jobs simultaneously is possible.

In backward extrusion, the area reduction is defined as follows:

$$RA\% = \frac{a}{A} (100)$$

where a is the cross sectional area of the punch and A the cross sectional area of the billet. The gap between the billet and the container is neglected because the accuracy of calculations was 0.1mm. Effect of this gap in area reduction is about 0.025-0.05 mm²; thus it had no considerable influence on the area reduction and was omitted in this equation.

In addition, friction factors for all simulations regarding AA1100-O were taken as 0.2 and for the AA2024-O, as 0.1 obtained from experimental data in references [2] and [4].

4. Analysis of the backward extrusion

Backward extrusion of shaped sections has been investigated in here using FEM simulation. A general schematic view of the backward extrusion process has been shown in figure 3.

Different cases of shaped extrusions simulated in this work have also been illustrated in figure 4.

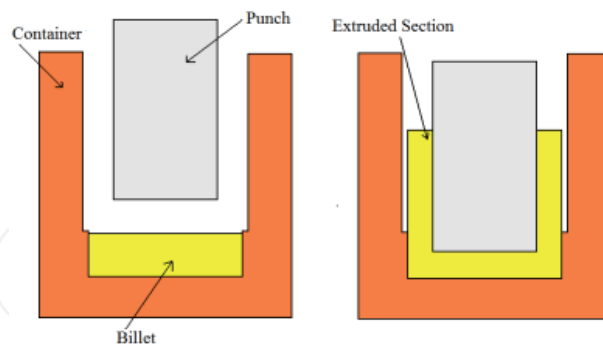


Fig. 3. A schematic view of the backward extrusion process

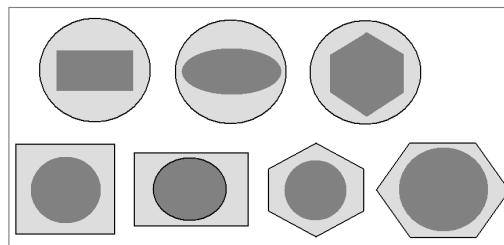


Fig. 4. Different cross sections simulated for the backward extrusion of shaped sections

ABAQUS\Explicit CAE commercial software was used for all simulations. The results are presented here according to the billet-punch shape (figure (4)).

4.1 Circular Billet-Elliptic Punch

4.1.1 Extrusion Load

Fig. 5 shows the effect of area reduction on the extrusion load for backward extrusion of internally elliptical-shaped tubes from round billets. The extrusion load increases with increasing reduction of area for a fixed aspect ratio and the given friction factor. FEM simulation results were compared with the experimental and theoretical values (Bae and Yang, 1992) and good agreements were found.

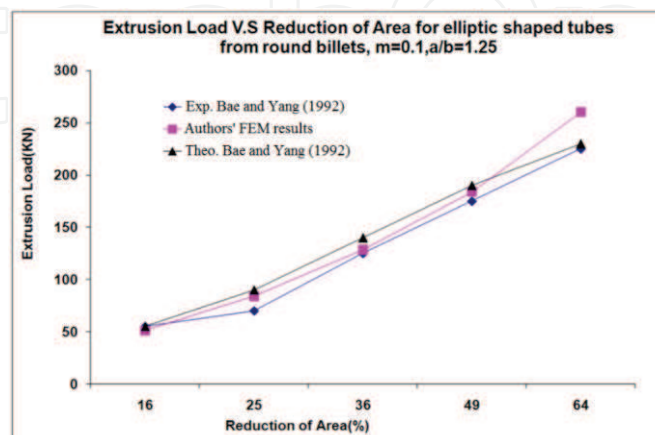


Fig. 5. Effect of area reduction on the extrusion load for the backward extrusion of elliptical section from round billet

For reduction of area of 36-49%, the extrusion loads were in good agreement with the experimental loads. The maximum difference between the value of the load obtained from the simulation and the experimental value was seen to be for the 64% area reduction.

The present simulation results for the extrusion load versus various aspect ratios in Fig. 6 are in good agreement with the experimental values and theoretical predictions (Bae and Yang, 1992). For aspect ratios of 1 to 1.3, the simulation results are closer to experimental ones. Fig. 7 shows the simulation results for the effect of friction factor on the extrusion load. For a given reduction of area and fixed aspect ratio, the extrusion load increases with the increase in the friction factor.

4.1.2 Distribution of Velocity and Configuration of the Free Surface of the Extruded Billet

The simulation results for the velocity distribution of the extruded billet are shown in Fig. 8-1 to Fig. 8-3 for different area reductions, aspect ratios, and friction factors, respectively. The effect of area reduction on the configuration of the free surface and velocity field contours of extruded billet for a given aspect ratio and the given friction factor are shown in Fig. 8-1. Fig. 8-2 shows the effect of aspect ratio on the configuration of the free surface and velocity field contribution of extruded billet for a fixed area reduction and the given friction factor. In Fig. 8-3 is shown the effect of friction factor on the configuration of the free surface and velocity field for the extruded billet having a constant aspect ratio and reduction of area. Diagrams of the velocity variables versus various area reductions, aspect ratios, and friction factors are shown in Fig. 9-1, Fig. 9-2 and Fig. 9-3, respectively.

In fig. 9-1, for a reduction of area smaller than 25%, the velocity could be seen to decrease with increasing reduction of area and for values of reduction of area 25-64%, it could be seen that the velocity increases with increasing reductions of area.

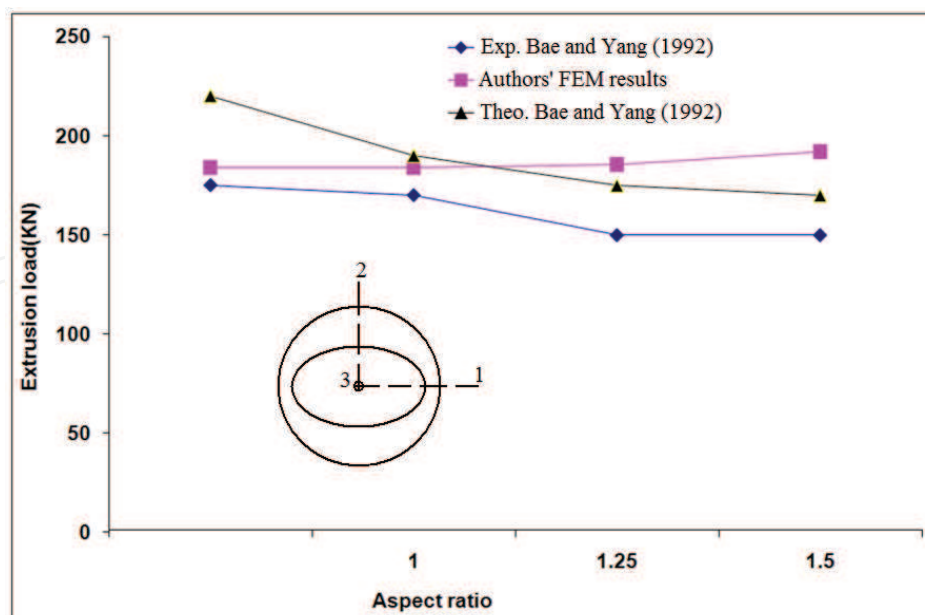


Fig. 6. Comparison of results with previous works for the backward extrusion of elliptical section from round billet

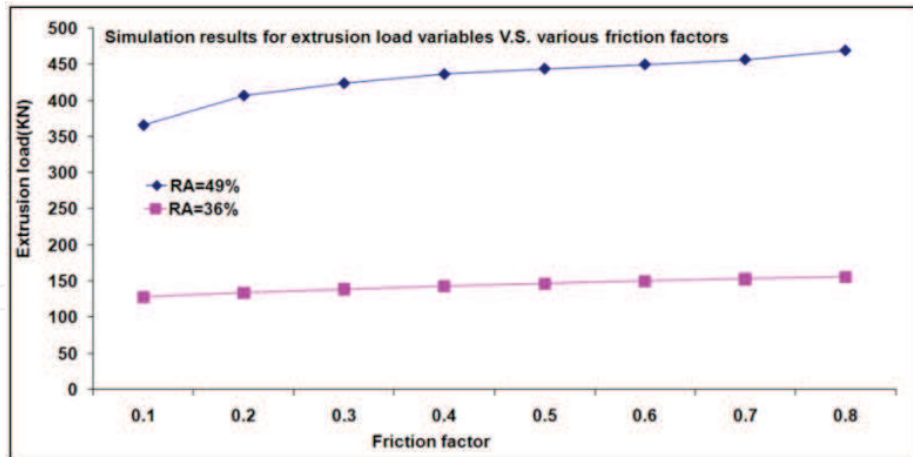


Fig. 7. Effect of frictional conditions on the extrusion load for the backward extrusion of elliptical section from round billet

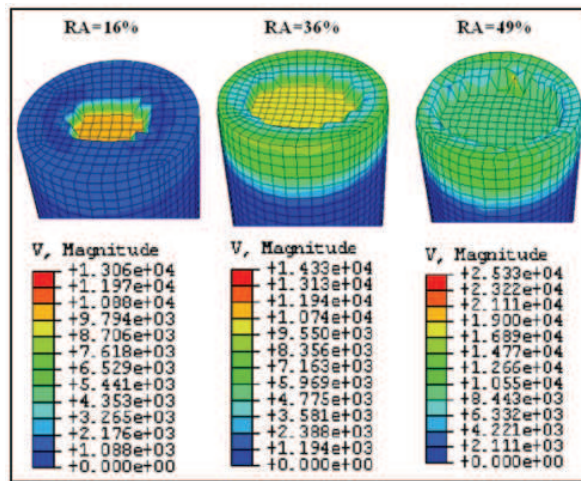


Fig. 8-1. Velocity distribution for the backward extrusion of elliptical sections from round billets-effect of reduction of area

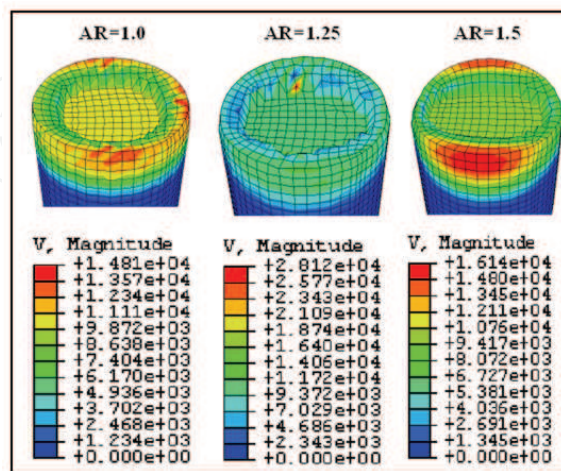


Fig. 8-2. Velocity distributions for the backward extrusion of elliptical sections from round billets-effect of aspect ratio

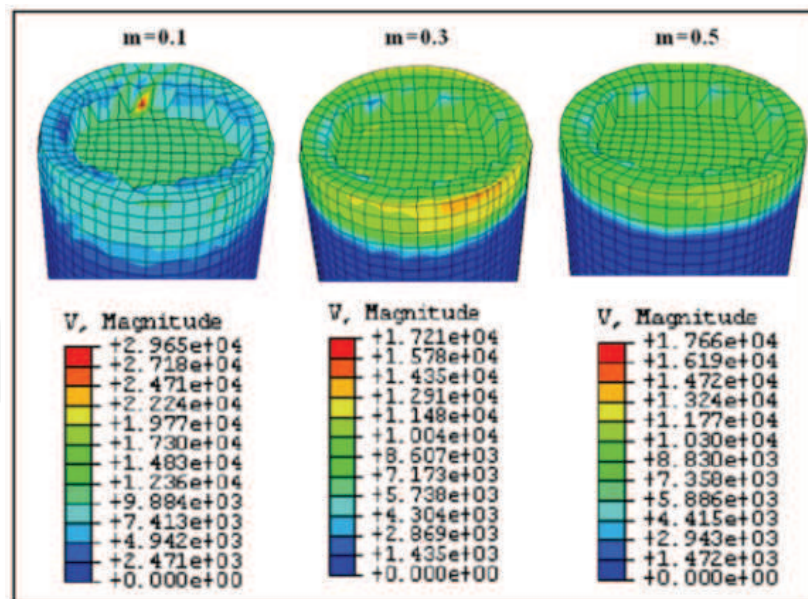


Fig. 8-3. Velocity distributions for the backward extrusion of elliptical sections from round billets-effect of frictional conditions

In Fig. 9-2, the effect of aspect ratio on the velocity has been shown. As could be seen from figure components of the velocity in directions 1 and 2 do not change appreciably with the aspect ratio while the component of the velocity in the axial direction (direction 3) changes very much with a variation in the aspect ratio and it is this component that has the major share of the total magnitude of the velocity. In Fig. 9-3, the effect of the friction factor on the velocity field has been shown. Except for very small values of the friction factor, there seems to be no appreciable difference between the different components of the velocity field. Simulation results for grid deformation could be seen in Fig. 10. Because of thinning in the work piece wall for a RA = 64%, the material flows toward punch and is distorted excessively; therefore, the material flow encounters difficulties.

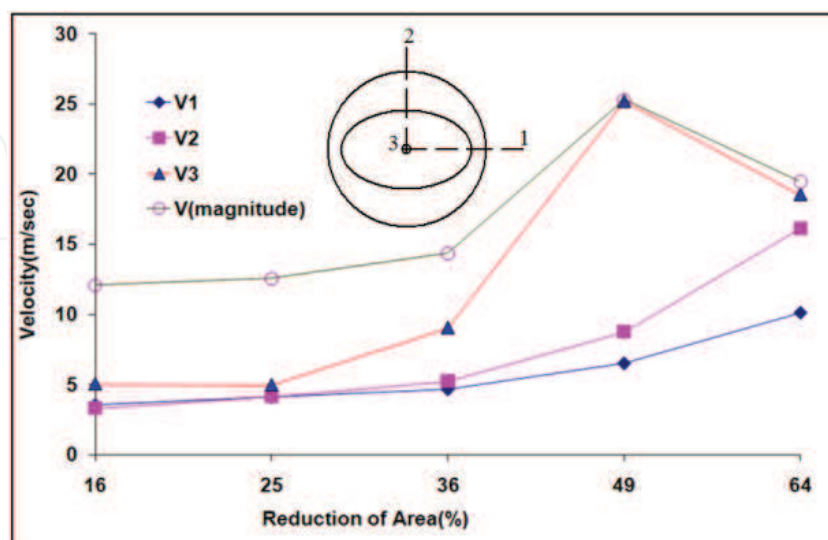


Fig. 9-1. Components of the velocity distribution- effect of reduction of area

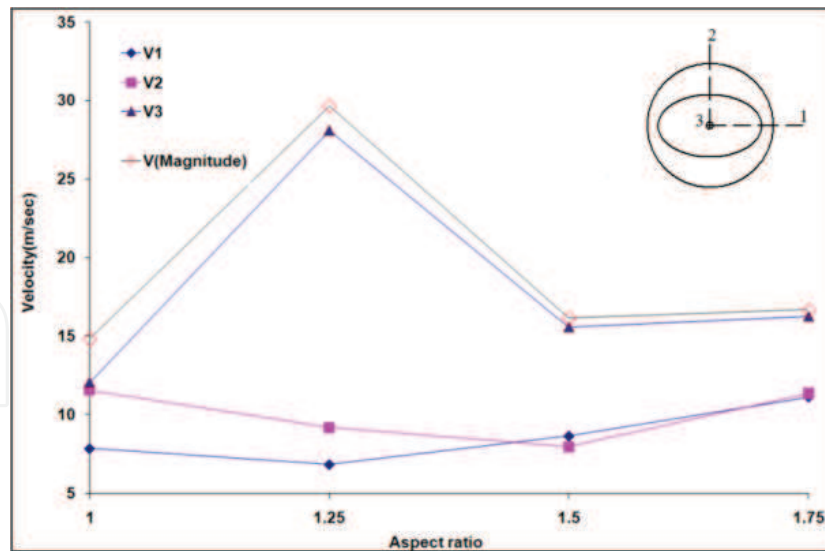


Fig. 9-2. Components of the velocity distribution- effect of aspect ratio

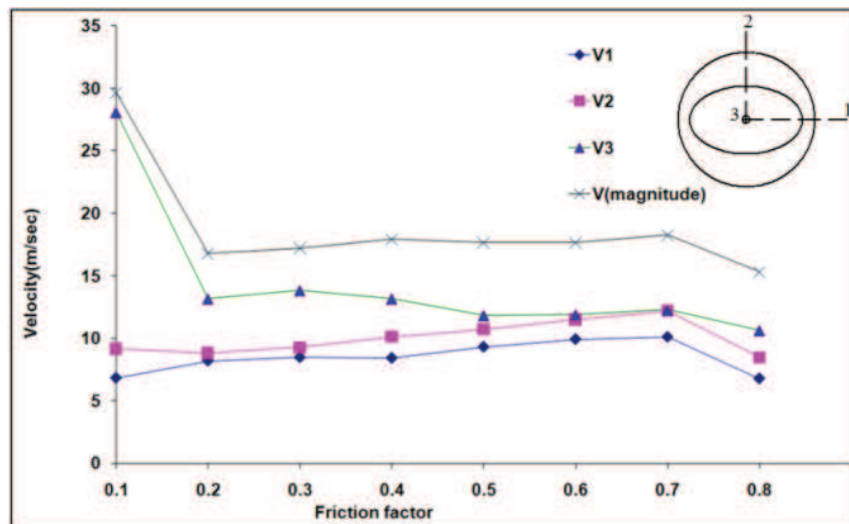


Fig. 9-3. Components of the velocity distribution- effect of frictional conditions

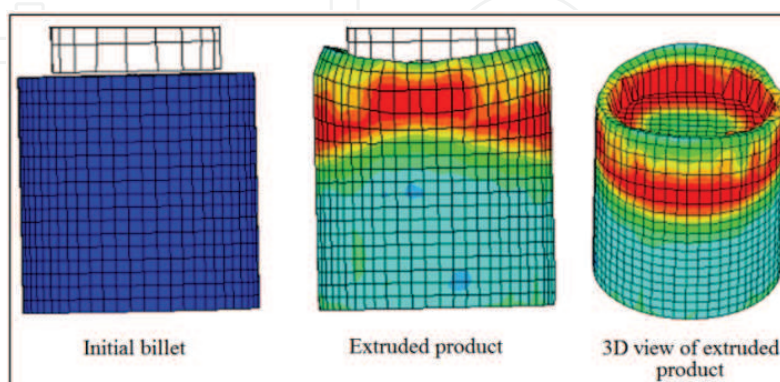


Fig. 10. Grid deformation for the backward extrusion of elliptical section from round billets

4.2 Circular Billet-Rectangular Punch Results

4.2.1 Extrusion Load

Fig. 11, Fig. 12 and Fig. 13 show the results of FEM simulation for internally rectangular sections from round billets. In Fig. 11, a graph of extrusion load versus reduction of area is given for the backward extrusion of internally rectangular sections from circular billets. Comparison of other theoretical and experimental results with the FEM simulation of the authors is also seen in this figure. Authors' results show better agreement with the experimental values at lower values of the reduction of area. In Fig. 12, a graph of extrusion load versus aspect ratio is given for the backward extrusion of internally rectangular sections from circular billets. Authors' results show better agreement with the experimental values at lower values of aspect ratio. The variation of the extrusion load with frictional conditions has been simulated and presented in figure 13 which shows the expected trend.

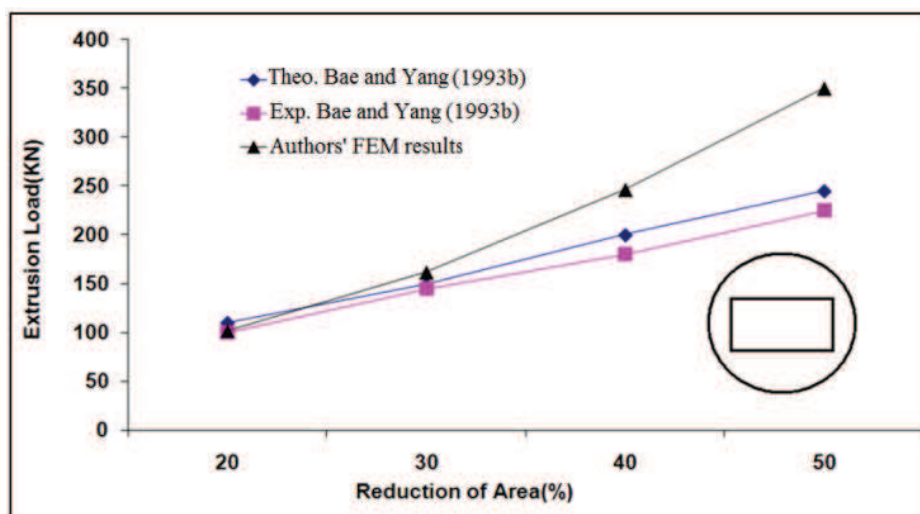


Fig. 11. Extrusion load versus reduction of area for the backward extrusion of rectangular sections from round billets

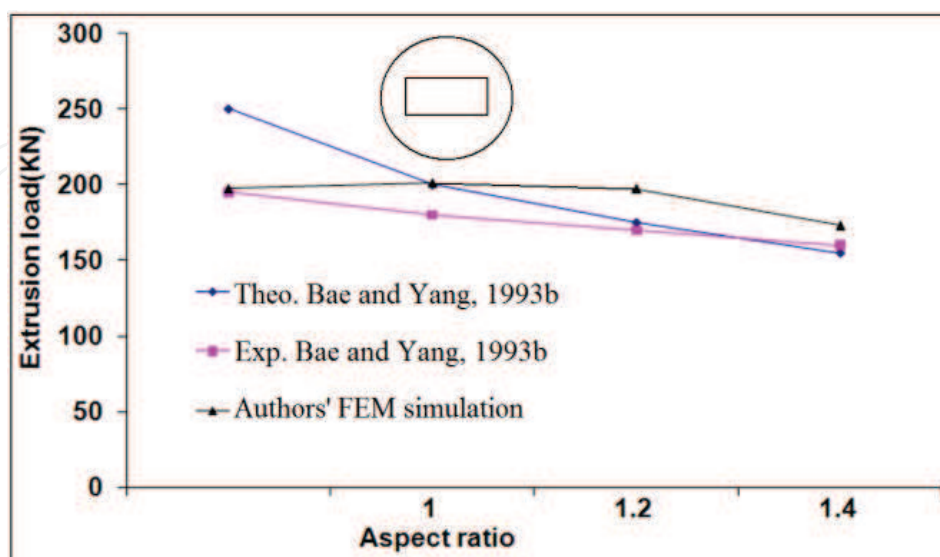


Fig. 12. Extrusion load versus aspect ratio for the backward extrusion of rectangular sections from round billets

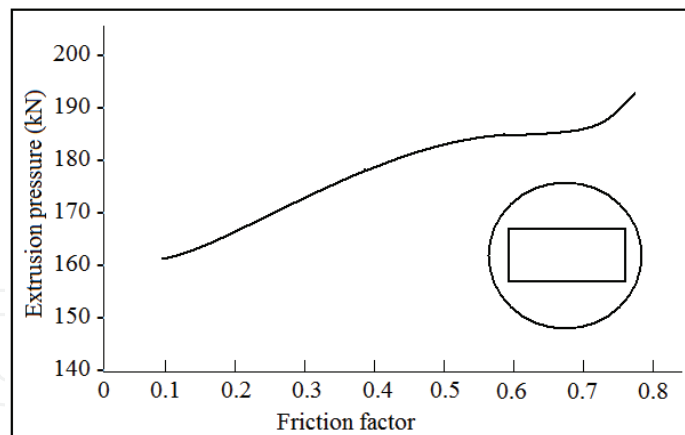


Fig. 13. Extrusion load versus friction factor for the backward extrusion of rectangular sections from round billets

3.2.2 Velocity Field Distribution

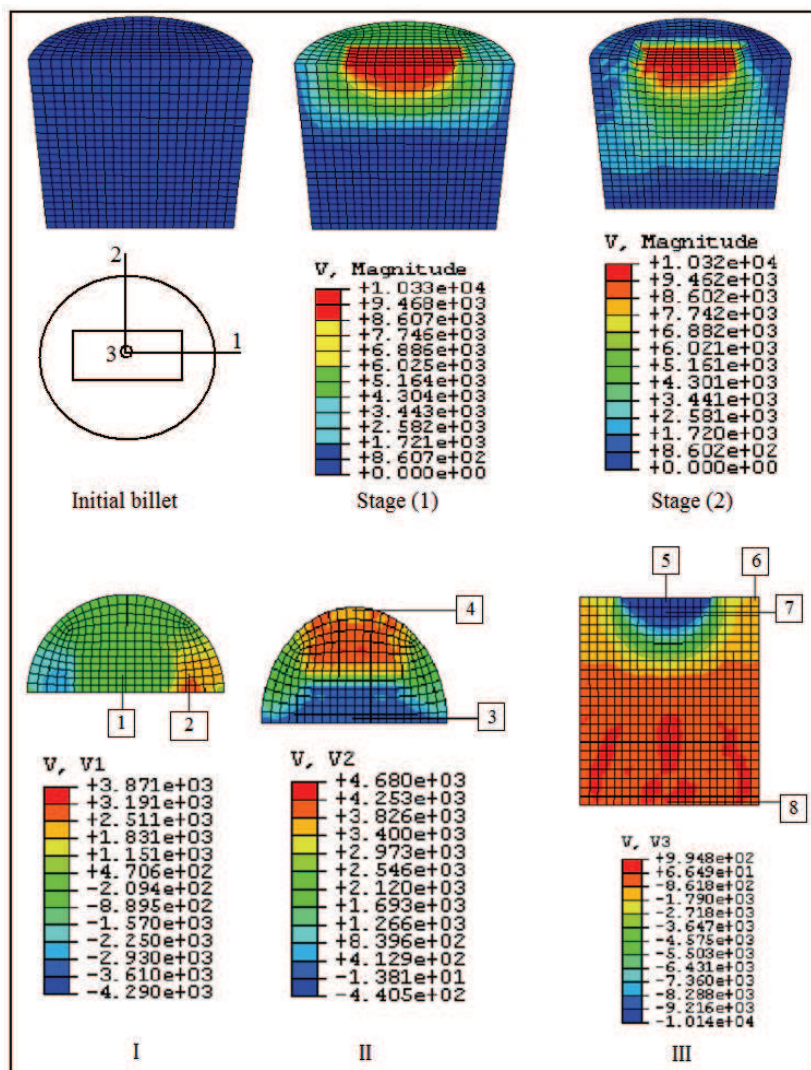


Fig. 14. Velocity distributions for the backward extrusion of rectangular section from circular billet

For the same extrusion, the grid deformation and spatial velocity distribution at nodes are also given in Fig. 14. Starting from the initial stage of the extrusion process and going through to the end, five different stages are observed. The values of velocity distributions in the part are also shown for each stage. The velocity field is shown by three directional velocities: V1, V2, and V3. The magnified figure of one stage for contour distribution of V1, V2, and V3 is shown in Fig. 14, respectively. The values of V1 were greater at locations nearer to the punch corner than elsewhere and it is lowest at the center of free surface of the extruded part at position (1). Also, V1 decreases from position (1) to (2), for the nodes near the wall of container. Values of V2 were greater at locations (3) and (4) and between these sections, V2 has the lowest value. The value of V3 was greatest at position (5) and decreases as one move toward (6), for the nodes of the work piece near the container wall. From position (7), near the free surface of workpiece toward position (8), for the nodes near the container lower section, V3 decreases gradually. These results were not obtained by other methods in other references.

4.3 Circular Billet-Hexagonal Punch Results

4.3.1 Stress and Strain Distribution

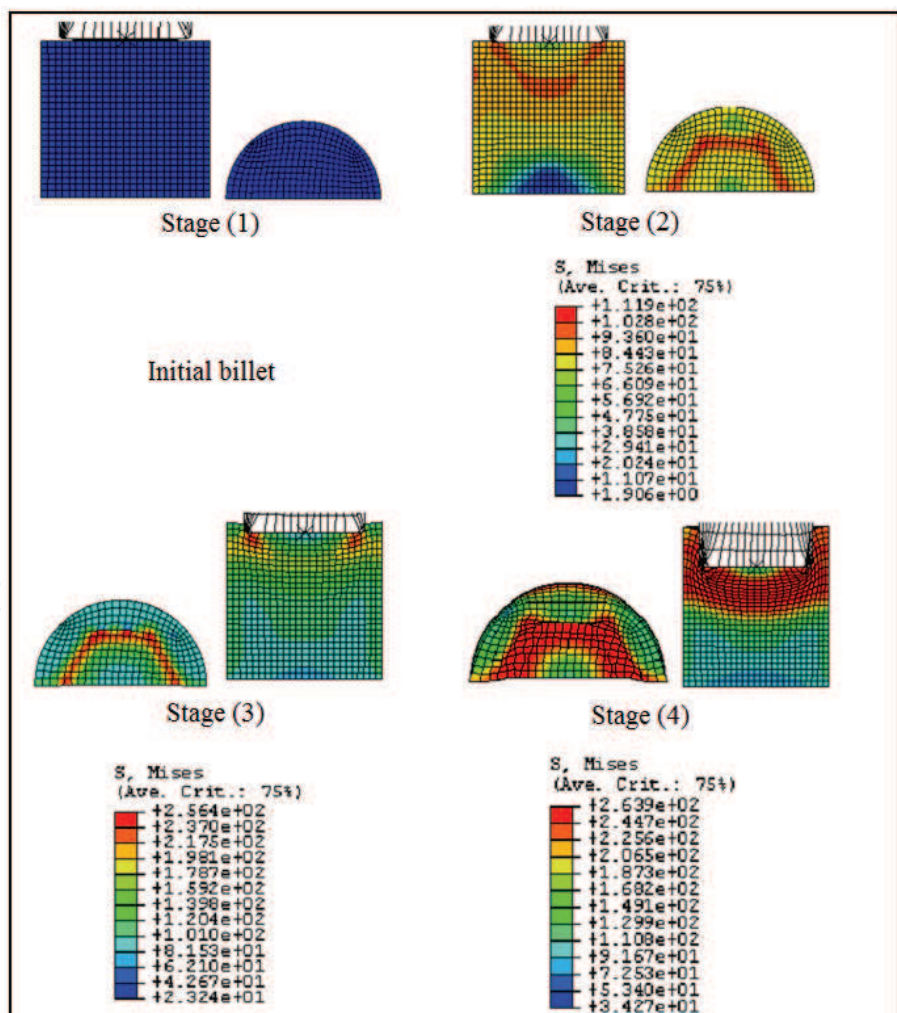


Fig. 15. Stress distribution for the backward extrusion of rectangular sections from round billets

For the same extrusion, the grid deformation and stress distribution are also given in Fig. 15. Starting from the initial stage of the extrusion process and going through to the end, four different stages are observed. The values of stress distribution in the part are also shown for each stage. A reduction of area of 49% was used for these simulations. It is illustrated that in which part of the billet the stress is greatest. The results for the equivalent strain distribution for the backward extrusion of internally hexagonal and externally circular shapes are shown in Fig. 16 for the four stages of the simulation. It could be seen that, as expected, the highest values of strain occur at where the deformation is at its highest level. As shown in these stages, because of maximum deformation in the surface of the work piece which is in contact with the corner of the punch, the plastic equivalent effective strain is greater than elsewhere. Also, in the initial stage of the process, contours of strains are distributed in broad areas and gradually decrease through the end of the process. The reason is that in the initial stage, with increasing stress, the plastic area develops and includes larger regions of the billet. However, after material flows and plastic deformation develops further, the deformation area is fixed and strains confine in the plastic areas. It should be mentioned that these results are very similar to those given in (Bae and Yang, 1993a).

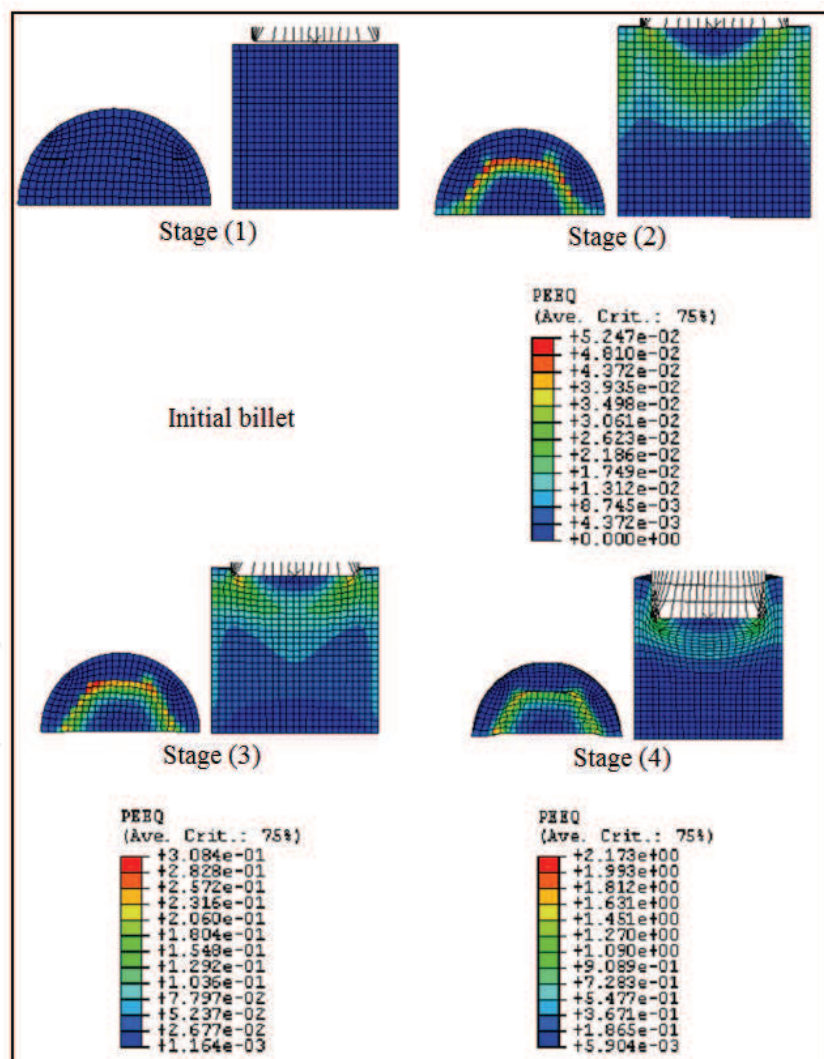


Fig. 16. Strain distribution for the backward extrusion of rectangular sections from round billets

4.4 Square Billet- Circular Punch Results

4.4.1 Extrusion load

Fig. 17 illustrates the area reduction influence on the extrusion load in backward extrusion process of internally circular-shaped tubes from square billets. The extrusion load increases with increasing area reduction for the given friction factor. Comparison of FE simulation with the experimental and theoretical values showed good agreement.

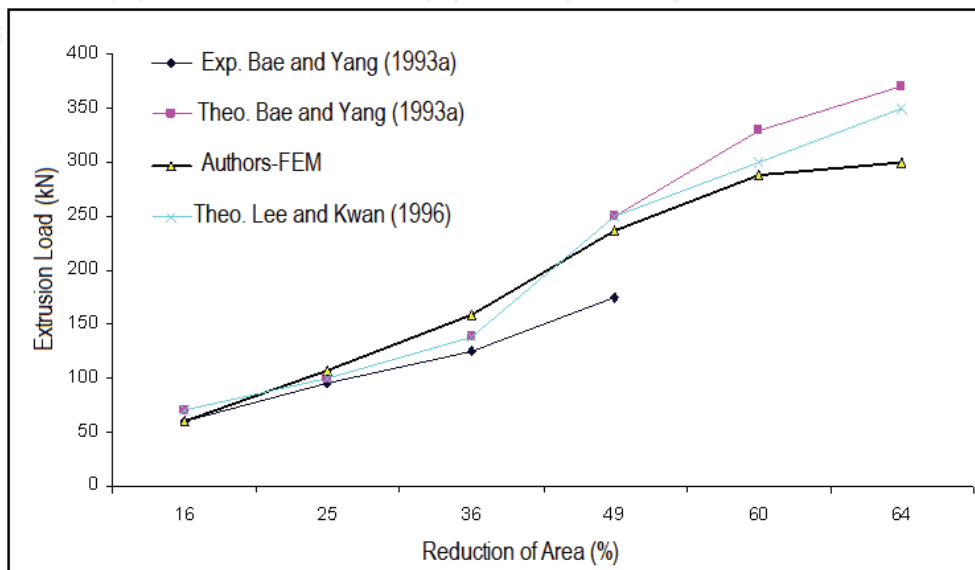


Fig. 17. Extrusion load versus reduction of area for the extrusion of internally circular and externally square shaped section

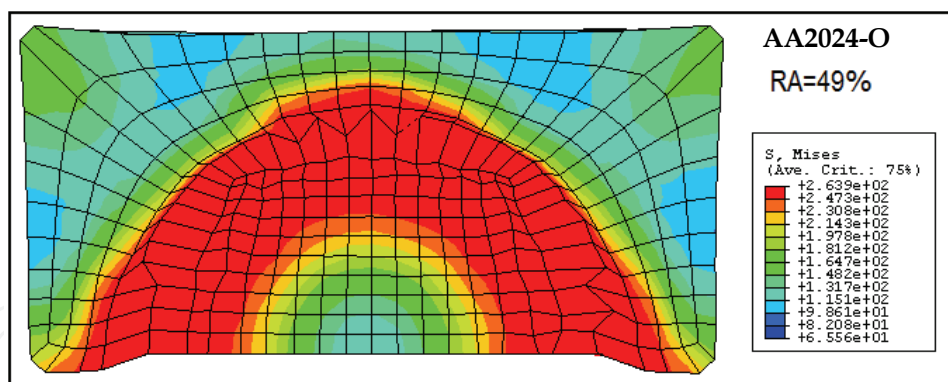


Fig. 18. Grid deformation for the extrusion of internally circular and externally square shaped sections

4.4.2 Stress distribution and grid deformation

A stress distribution contour of the backward extrusion of circular tubes with square sections is indicated in Fig. 18 as FE simulation result. The Von-Mises stress increases from the center of the section towards the internal wall of work piece then it diminishes toward external wall. It seems that because of material flows under the punch and the frictional velocity discontinuities, the stress increases. However as the material flow develops further towards the external surface it passes over the punch area and since there are no obstacle in

the path of the material flow it decreases at this position. In the vertical direction of the deformation area and under the punch, the conical shaped dead zone is created which acts rigidly and moves downward with the punch like part of it.

4.5 Hexagonal Billet- Circular Punch Results

4.5.1 Distribution of velocity and configuration of the free surface of the extruded billet

The Simulation results for the influence of the reduction in area on the velocity field have been shown in Fig. 19. It could be observed that as the reduction in area increases from 16

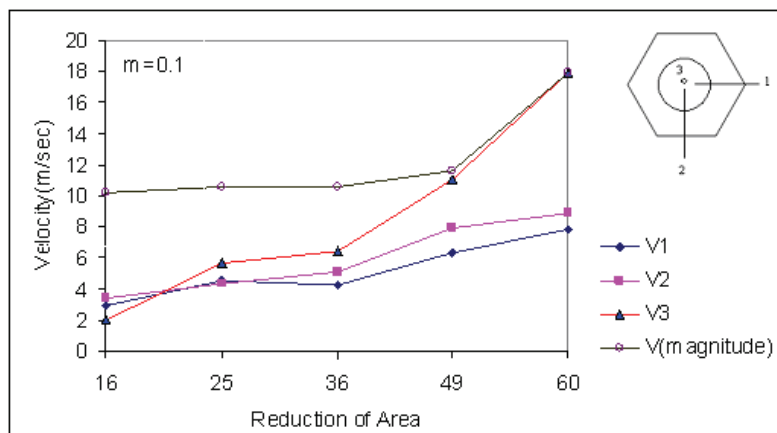


Fig. 19. Velocity components for the extrusion of internally circular and externally hexagonal shaped sections

to 49 percent, all three components of velocity (V1, V2, and V3) have similar magnitudes but at higher reductions the component V3 suddenly rises sharply. The reason for this seems to be the shape of the circular tube which is being extruded. At lower reductions, the thickness of tube walls is such that the flow of material happens evenly in all directions. However at 60% area reduction, it is clear that the components of velocity in the directions (1) and (2) follow the same trend as before while the component of velocity in direction (3) increases with sharp trend. This phenomenon can be explained by thinning of extruded wall which causes faster flow of material in this direction.

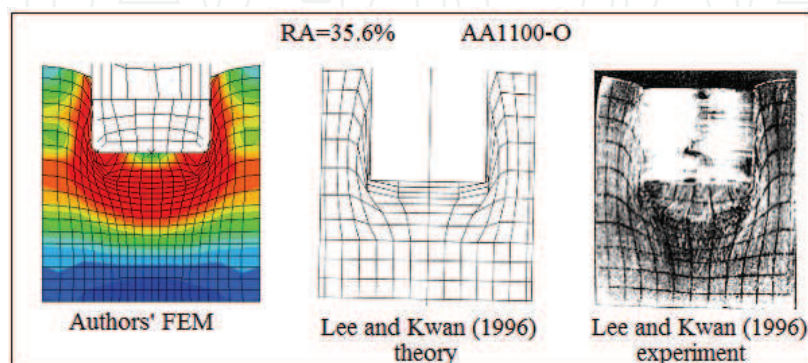


Fig. 20. Grid deformation for the extrusion of internally circular and externally hexagonal shaped sections

4.5.2 Grid deformation

Fig. 20 illustrates the grid deformation for the backward extrusion of internally circular shaped tubes from hexagonal billets, using FE simulation as compared with previous experimental and theoretical results (Lee and Kwan, 1996). FE outcomes are closer to the experimental results than the upper bound solutions. As illustrated in the figure, maximum deformation is observed in the corners and walls of the workpiece.

4.6 Rectangular Billet- Circular Punch Results

4.6.1 Strain distribution

Four stages of backward extrusion process have been simulated in the Fig. 21. Plastic equivalent effective strain contours of internally circular and externally rectangular shaped tubes are shown in this figure. It could be seen that, as expected, the highest values of strains occur at where the maximum deformation exists. The plastic equivalent effective strain in the areas where workpiece contacts with punch corner is greater than elsewhere. Consequently, maximum deformation happens in the zone of the workpiece in contact with the punch corner. In addition, in the initial stage of the process, contours of strains are distributed in broad areas and gradually decrease through the end of process.

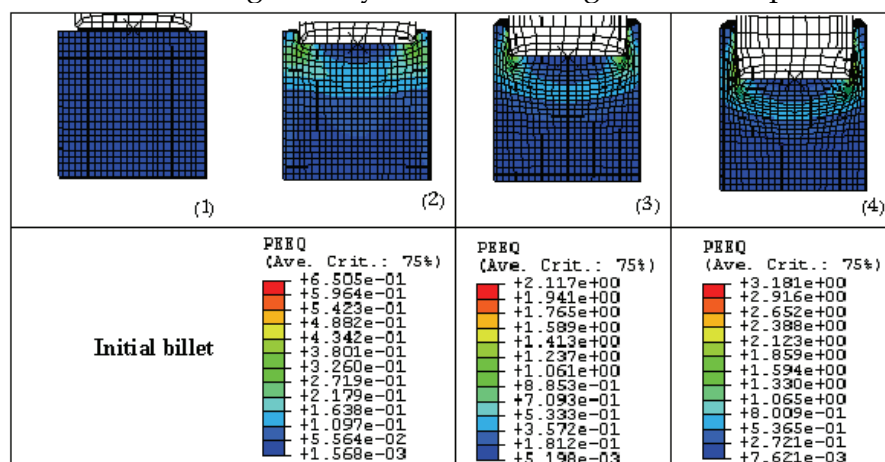


Fig. 21. Four stages of backward extrusion process for a rectangular billet and a circular punch giving the effective strain contours

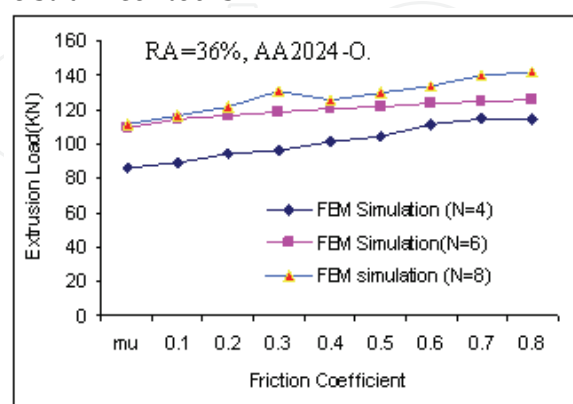


Fig. 22 Comparison of results for the backward extrusion of different polygonal sections.

This is because, in the initial stage, with increasing stress, the plastic area develops and includes larger region of billet, however, after material flows, there is no need for the load to increase and the deformation area is fixed and strains are confined to smaller plastic areas.

4.7 Extrusion load variables versus friction factor for polygonal billets and circular punches

The results of FE simulation for backward extrusion of internally circular shaped tubes from polygonal billets are depicted in figure 22 as the diagram of extrusion load versus friction factor. It could be concluded that with increasing the number of polygonal edges, the extrusion load goes up. This is due to the increase of the area of contact of the billet and the container, having in mind that the reduction of area has been kept constant; hence the friction force raises and causes the extrusion load to increase.

5. Conclusions

Finite element simulation of the backward extrusion process was carried out for shaped sections with internally elliptical, rectangular, hexagonal and externally circular shapes and also for the internally circular and externally polygonal sections.

- The 3D simulation predictions for the extrusion force for lower reduction of areas were closer to experimental observations whereas for higher reductions they were further apart.
- Some results such as the velocity distribution during different stages of the extrusion process for rectangular tubes and other results such as extrusion load, stress, and strain distribution for hexagonal tubes were also obtained which were not given in the previous work.
- The 3D velocity field distribution and the free surface configurations were presented by this simulation.
- It was concluded from the results given here that hollow sections with large reductions and thin walls are more prone to distortions due to the large differences in the components of velocity in different directions.
- A detailed analysis of strain, stress and velocity field for the backward extrusion of shaped section was presented which assisted a better understanding of the process.

6. Future Work

Backward extrusion of thin sections requires high loads and precision tooling; special designs in tooling could reduce the extrusion load considerably and eliminate the requirements for the high precision tooling. Therefore investigation into the tooling design and process design could be done by FEM simulation to evaluate the feasibility of such ideas before embarking on experimenting and manufacturing. This is currently under investigation by the authors.

7. References

- Abrinia, K. and Orangi, S. (2007). A Finite Element Simulation for the Backward Extrusion of Internally Hollow Circular Sections from Polygonal Billets, *Journal of Faculty of Engineering of the University of Tehran*, 40(6), 771-780,1026-0803.
- Abrinia, K. and Gharibi, K. (2008). An investigation into the extrusion of thin walled cans, *Int J Mater Form*, Suppl 1:411-414, 1960-6206.
- Abrinia K. and Orangi S., (2009) Investigation of Process Parameters for the Backward Extrusion of Arbitrary-Shaped Tubes from Round Billets Using Finite Element Analysis, *J Mat Eng Perform*, 18, 1201-1208, 1059-9495.
- Bae, W.B. and Yang, D.Y. (1992). An Upper-Bound Analysis of the Backward Extrusion of Internally Elliptic-Shaped Tubes from Round Billets, *J Mat Proc Tech*, 30(1-2), 13-20, 0924-0136.
- Bae, W.B. and Yang, D.Y. (1993-a). An Analysis of Backward Extrusion of Internally Circular-Shaped Tubes from Arbitrarily-Shaped Billets by the Upper-Bound Method, *J Mat Proc Tech.*, 36(2), 175-185, 0924-0136.
- Bae, W.B. and Yang, D.Y. (1993-b). An Upper-Bound Analysis of the Backward Extrusion of Tubes of Complicated Internal Shapes from Round Billets, *J Mat Proc Tech*, 1993, 36(2), 157-173, 0924-0136.
- Bakhshi-Jooybari, M., Saboori, M., Hosseinipour, S.J., Shakeri, M. and Gorji, A., (2006). Experimental and numerical study of optimum die profile in backward rod extrusion, *J Mat Proc Tech*, 177, 596-599, 0924-0136.
- Guo, Y.M., Yokouchi, Y. and K. Nakanishi, (2000). Hot Backward Extrusion Comparative Analyses by a Combined Finite Element Method, *Int J Mech Sci*, 42, 1867-1885.
- Im, Y.T., Kang, S.-H., Cheon, J.-S. and Lee, J.H. (2004). Finite element simulation of tip test with an aluminum alloy, *J Mat Proc Tech*, 157-158, 171-176, 0924-0136.
- Lee, R.-S., and Kwan, C.T. (1996). A Modified Analysis of the Backward Extrusion of Internally Circular-Shaped Tubes from Arbitrarily Shaped Billets by the Upper-Bound Elemental Technique, *J Mat Proc Tech*, 59, 351-358, 0924-0136.
- Lin, Y.T. and Wang, J.P. (1997). A New Upper-Bound Elemental Technique Approach, *J Comput Struct*, 65(4), 601-611, 0045-7949.
- Long, H. (2006), Quantitative evaluation of dimensional errors of formed components in cold backward cup extrusion, *J Mat Proc Tech*, 177, 591-595, 0924-0136.
- Moshksar, M.M. and Ebrahimi, R. (1998) An Analytical Approach for Backward Extrusion Forging of Regular Polygonal Hollow Components, *Int J Mech Sci*, 40(12), 1247-1263, 1867-1885.
- Orangi, S. and Abrinia, K. (2005) 3D simulation of backward extrusion process for production of internally shaped circular tubes sections from arbitrarily shaped tubes, *ISME International Conference*, Isfahan University of technology, Isfahan, Iran, May 2005.
- Saboori, M., Bakhshi-Jooybari, M., Noorani-Azad, M. and Gorji, A., (2006). Experimental and numerical study of energy consumption in forward and backward rod extrusion, *J Mat Proc Tech*, 177, 612-616, 0924-0136.
- Shin, T.J., Lee, Y.H., Yeom, J.T., Chung, S.H., Hong, S.S., Shim, I.O., Park, N.K., Lee, C.S. and Hwang, S.M. (2005). Process optimal design in non-isothermal backward extrusion of a titanium alloy by the finite element method, *Comput Methods Appl Mech Engrg*, 194, 3838-3869, 0045-7825.

Uyyuru, R.K.U. and Valberg, H., (2006). Physical and numerical analysis of the metal flow over the punch head in backward cup extrusion of aluminum, *J Mat Proc Tech*, 172, 312-318, 0924-0136.

Wriggers, Peter (2008) *Nonlinear Finite Element Method*, Springer, ISBN-10: 3540710000.

IntechOpen

IntechOpen



Finite Element Analysis

Edited by David Moratal

ISBN 978-953-307-123-7

Hard cover, 688 pages

Publisher Sciyo

Published online 17, August, 2010

Published in print edition August, 2010

Finite element analysis is an engineering method for the numerical analysis of complex structures. This book provides a bird's eye view on this very broad matter through 27 original and innovative research studies exhibiting various investigation directions. Through its chapters the reader will have access to works related to Biomedical Engineering, Materials Engineering, Process Analysis and Civil Engineering. The text is addressed not only to researchers, but also to professional engineers, engineering lecturers and students seeking to gain a better understanding of where Finite Element Analysis stands today.

How to reference

In order to correctly reference this scholarly work, feel free to copy and paste the following:

Karen Abrinia, and Sakineh Orangi (2010). Numerical Study of Backward Extrusion Process Using Finite Element Method, Finite Element Analysis, David Moratal (Ed.), ISBN: 978-953-307-123-7, InTech, Available from: <http://www.intechopen.com/books/finite-element-analysis/numerical-study-of-backward-extrusion-process-using-finite-element-method>

INTECH
open science | open minds

InTech Europe

University Campus STeP Ri
Slavka Krautzeka 83/A
51000 Rijeka, Croatia
Phone: +385 (51) 770 447
Fax: +385 (51) 686 166
www.intechopen.com

InTech China

Unit 405, Office Block, Hotel Equatorial Shanghai
No.65, Yan An Road (West), Shanghai, 200040, China
中国上海市延安西路65号上海国际贵都大饭店办公楼405单元
Phone: +86-21-62489820
Fax: +86-21-62489821

© 2010 The Author(s). Licensee IntechOpen. This chapter is distributed under the terms of the [Creative Commons Attribution-NonCommercial-ShareAlike-3.0 License](#), which permits use, distribution and reproduction for non-commercial purposes, provided the original is properly cited and derivative works building on this content are distributed under the same license.

IntechOpen

IntechOpen